ISSN 1674-1056
http://cpb.iphy.ac.cn
http://iopscience.iop.org/cpb
中国物理 B
Chinese Physics
中国物理
Chinese Physics B

Comparison of the sensitivities for atom interferometers in two different operation methods

Xiao-Chun Duan(段小春), De-Kai Mao(毛德凯), Xiao-Bing Deng(邓小兵), Min-Kang Zhou(周敏康), Cheng-Gang Shao(邵成刚), Zhu Zhu(祝竺), Zhong-Kun Hu(胡忠坤)
Citation: Chin. Phys. B . 2018, 27(1): 013701. **doi:** 10.1088/1674-1056/27/1/013701

Journal homepage: http://cpb.iphy.ac.cn; http://iopscience.iop.org/cpb

What follows is a list of articles you may be interested in

Common-mode noise rejection using fringe-locking method in WEP test by simultaneous dual-species atom interferometers

Xiao-Bing Deng(邓小兵), Xiao-Chun Duan(段小春), De-Kai Mao(毛德凯), Min-Kang Zhou(周敏康), Cheng-Gang Shao(邵成刚), Zhong-Kun Hu(胡忠坤)
Chin. Phys. B . 2017, 26(4): 043702. **doi:** 10.1088/1674-1056/26/4/043702

Investigation of the thermal adaptability for a mobile cold atom gravimeter

Qi-Yu Wang(王启宇), Zhao-Ying Wang(王兆英), Zhi-Jie Fu(付志杰), Qiang Lin(林强)
Chin. Phys. B . 2016, 25(12): 123701. **doi:** 10.1088/1674-1056/25/12/123701

Rapid extraction of the phase shift of the cold-atom interferometer via phase demodulation

Cheng Bing, Wang Zhao-Ying, Xu Ao-Peng, Wang Qi-Yu, Lin Qiang
Chin. Phys. B . 2015, 24(11): 113704. **doi:** 10.1088/1674-1056/24/11/113704

Precision measurement with atom interferometry

Wang Jin
Chin. Phys. B . 2015, 24(5): 053702. **doi:** 10.1088/1674-1056/24/5/053702

Comparison of the sensitivities for atom interferometers in two different operation methods*

Xiao-Chun Duan(段小春)[1], De-Kai Mao(毛德凯)[1], Xiao-Bing Deng(邓小兵)[1], Min-Kang Zhou(周敏康)[1], Cheng-Gang Shao(邵成刚)[1], Zhu Zhu(祝竺)[2], and Zhong-Kun Hu(胡忠坤)[1,†]

[1] *MOE Key Laboratory of Fundamental Physical Quantities Measurements, Hubei Key Laboratory of Gravitation and Quantum Physics, School of Physics, Huazhong University of Science and Technology, Wuhan* 430074, *China*

[2] *Shanghai Institute of Satellite Engineering, Shanghai* 201109, *China*

(Received 3 August 2017; revised manuscript received 20 September 2017; published online 17 November 2017)

We investigated the sensitivities of atom interferometers in the usual fringe-scanning method (FSM) versus the fringe-locking method (FLM). The theoretical analysis shows that for typical noises in atom interferometers, the FSM will degrade the sensitivity while the FLM does not. The sensitivity-improvement factor of the FLM over the FSM depends on the type of noises, which is validated by numerical simulations. The detailed quantitative analysis on this fundamental issue is presented, and our analysis is readily extendable to other kinds of noises as well as other fringe shapes in addition to a cosine one.

Keywords: atom interferometer, fringe locking, fringe scanning, sensitivity

PACS: 37.25.+k, 07.05.Kf **DOI:** 10.1088/1674-1056/27/1/013701

1. Introduction

Atom interferometers have important applications in fundamental physics, such as the measurement of fine structure constants,[1–5] the determination of gravitational constant G,[6–12] and the test of general relativity.[13–17] They are also used in atom clocks,[18–24] atom magnetic gradiometers,[25,26] atom gravimeters,[27–36] etc. In these applications, the interference pattern is usually manifested as a cosine variation of the transition probability, and the method to extract the phase from the cosine fringe is crucial for the interferometer's performance. Usually, a full cosine fringe is obtained by scanning a controllable phase, as shown in Fig. 1(a). The interested information is then acquired by a cosine fitting. Alternatively, the fringe-locking method (FLM) can be adopted,[18,29,36–38] which ensures measurements are always performed at the mid-fringe, as shown in Fig. 1(b). Then the interested phase can be obtained from the modulating center φ^0.

There are several advantages offered by the FLM compared with the usual fringe-scanning method (FSM). Firstly, it is capable of increasing the sampling rate by about one order of magnitude.[36] This is helpful in monitoring fast temporal variable signals, which may find applications in future space missions. Secondly, the measurement equation can be linearized at mid-fringe, which allows a direct extraction of the interested information. This linearization may also make the interferometry-process related analysis simple.[27] Thirdly, the data at the mid-fringe are more sensitive to phase variation than those at other points throughout the full fringe. This implies a possible sensitivity improvement by the FLM over the FSM in resolving the interferometry phase shift. In this paper we focus on the third issue, since in many measurements the sensitivity is most concerned with pursuing the precision within a certain measurement time.

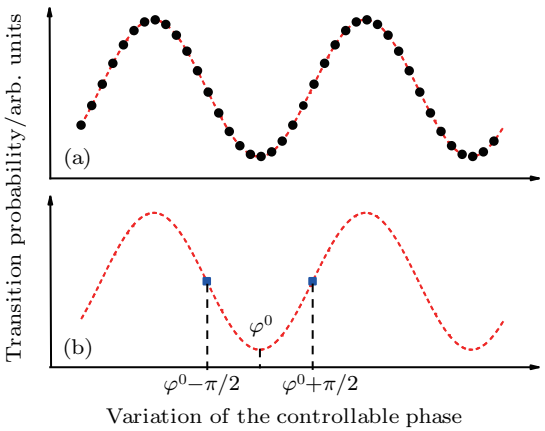


Fig. 1. (color online) Different methods to operate the interferometer: (a) recording full fringes, and (b) performing measurements at mid-fringe. In the fringe-scanning method, the phase is scanned step by step, while in the fringe-locking method, the phase is modulated by $\pm\pi/2$ with respect to an appropriate center denoted as φ^0 here. The dashed lines are here to guide the eyes.

At the mid-fringe, the slope is indeed maximal throughout the full fringe, however the corresponding noise may also be maximal. Thus it is supposed that the possible improvement depends on detailed noises. Here the sensitivity-improvement factor for the FLM over the FSM is investigated for three typical noises in atom interferometers, namely, fringe-site inde-

*Project supported by the National Natural Science Foundation of China (Grant Nos. 41127002, 11574099, 41504034, and 11474115) and the National Basic Research Program of China (Grant No. 2010CB832806).

†Corresponding author. E-mail: zkhu@hust.edu.cn

© 2018 Chinese Physical Society and IOP Publishing Ltd

pendent noise, atomic shot noise, and phase noise. The result shows that the FLM indeed affords an improvement of the sensitivity and the corresponding improvement factors are $\sqrt{2}$, $\sqrt{3/2}$ to $\sqrt{2}$ (depending on the fringe visibility), and $\sqrt{3/2}$ for the three kinds of noises, respectively. Furthermore, we extend the analysis to coupled atom interferometers, and find that an improvement with a factor greater than $\sqrt{2}$ may be expected for the common fringe-site independent noises. This is the first detailed quantitative analysis on this issue, which helps to design the experimental setup, understand the measurement result, and distinguish the dominant noise for the interferometers.

2. Approaches illumination

In atom interferometers, the direct output signal is given by the transition probability P between the two ground levels of the atom, which is usually a cosine function of the interferometry phase shift, namely, $P = A + B\cos(\varphi + \varphi_{\rm m})$. In the above expression, A is the fringe offset, B is the fringe amplitude, φ stands for the controllable phase shift, and $\varphi_{\rm m}$ indicates the phase shift induced by the interested physical quantity to be measured. In the ideal case of many atom interferometers, both A and $|B|$ equal to 1/2. In practice, the exact value of A does not matter much in the acquisition of $\varphi_{\rm m}$, and $|B|$ is usually smaller than 1/2 due to various experimental imperfections. Thus for simplicity, in this work, the transition probability is expressed as

$$P = (1 - \eta\cos(\varphi + \varphi_{\rm m}))/2, \tag{1}$$

where η $(0 < \eta \leq 1)$ is the fringe visibility.

In the FSM, φ is scanned step by step to acquire a full fringe, as shown in Fig. 1(a). Then η and $\varphi_{\rm m}$ can be obtained by a cosine fitting based on the least-square residual (LSR) method.[39] This technique finds the best estimation of η and $\varphi_{\rm m}$ that minimize the sum of the squared residuals, namely,

$$\min \sum_{i=1}^{N} \left(\frac{1 - \eta\cos(\varphi_i + \varphi_{\rm m})}{2} - p_i \right)^2, \tag{2}$$

where φ_i denotes the value of φ in the i-th step during a full fringe scan, p_i stands for the corresponding measured transition probability in the presence of noises, and N denotes the total step number for one full fringe. The precision of the obtained $\varphi_{\rm m}$ can be estimated from the propagation of errors as

$$\sigma_{\varphi_{\rm m}}^2 = \sum_{i=1}^{N} (\partial_{p_i}\varphi_{\rm m})^2 \sigma_{p_i}^2, \tag{3}$$

where σ_{p_i} denotes the variance of p_i and the independence of σ_{p_i} from each other has been assumed. The error propagation factor $\partial_{p_i}\varphi_{\rm m}$ depends on the way of extracting $\varphi_{\rm m}$ from p_i, which in a usual case changes along the fringe. For the cosine fitting method, the calculation of $\partial_{p_i}\varphi_{\rm m}$ is presented in Appendix A. σ_{p_i} may also depend on the fringe site. Here we take a simple case as an example to illustrate our analysis approach. We consider that the dominated noise of the atom interferometry is fringe-site independent, namely, σ_{p_i} is constant throughout the whole fringe. Thus the explicit expression of the precision for $\varphi_{\rm m}$ is

$$\begin{aligned}&(\sigma_{\varphi_{\rm m}}^{\rm FS}(N))^2 \\ &= \frac{4\sigma_P^2}{\eta^2} \frac{\sum_{i=1}^{N} \cos^2\phi_i}{\left[\sum_{i=1}^{N} \cos^2\phi_i\right] \times \left[\sum_{i=1}^{N} \sin^2\phi_i\right] - \left[\sum_{i=1}^{N} \cos\phi_i \sin\phi_i\right]^2},\end{aligned} \tag{4}$$

where ϕ_i is the temporal substitution for $\varphi_i + \varphi_{\rm m}$ for simplification, and the superscript FS is the abbreviation of fringe scanning. In practical scanning, φ is uniformly scanned over 2π. In order to obtain an analytic expression of Eq. (4), it is further assumed that φ is scanned with such an infinitesimal step that the summation can be approximated by an integral. The corresponding result is

$$\sigma_{\varphi_{\rm m}}^{\rm FS}(N) = 2\sqrt{2}\sigma_P/\eta\sqrt{N}. \tag{5}$$

For other kinds of noises, the precision of the obtained $\varphi_{\rm m}$ can be similarly estimated as long as the detailed dependence of σ_{p_i} on the fringe site is accounted for.

In the FLM, the appropriate value of φ, denoted as φ^0, is firstly found to make $\varphi^0 + \varphi_{\rm m} \sim 2n\pi$ (n is an integer). Then φ is modulated by $\pm\pi/2$ with respect to φ^0 so that the measurement is always performed at the mid-fringe, alternately to the right and to the left side of the central fringe, as shown in Fig. 1(b). The corresponding transition probabilities for every two adjacent measurements are expressed as

$$\begin{cases} P_{2l} = (1 - \eta\cos(\varphi_l^0 + \varphi_{\rm m} - \pi/2))/2, \\ P_{2l+1} = (1 - \eta\cos(\varphi_l^0 + \varphi_{\rm m} + \pi/2))/2, \end{cases} \tag{6}$$

where the subscript l denotes the index of modulating cycles. According to the linear approximation of Eq. (6) at the mid-fringe, the correction of φ^0 for the $l+1$ cycle can be expressed as

$$\delta(\varphi^0) = -(P_{2l+1} - P_{2l})/\eta. \tag{7}$$

This real-time feedback ensures that the measurements are always performed at the mid-fringes, whether or not there is a change of the interested quantity or an external disturbance. For FLM, the fringe visibility η (generally, the fringe amplitude) must be known in advance to perform the feedback, which is further assumed to be constant in the measurements. It must also be noted that, in order to lock the fringe, the noises should be suppressed to a level such that the recorded transition probabilities are not far from the mid-fringe. Once the

correction is made to form a closed feedback loop, the equation $\varphi^0+\varphi_{\rm m}=2n\pi$ is supposed to be tenable. Thus the knowledge of $\varphi_{\rm m}$ can be obtained from the value of φ^0, and the fluctuation of the recorded φ^0 directly reflects the precision of $\varphi_{\rm m}$. The variance of P at the mid-fringe is denoted as $\sigma_P^{\rm mid}$ here. According to Eq. (7), for FLM, the precision of $\varphi_{\rm m}$ for a single modulating cycle can be expressed as $\sigma_{\varphi_{\rm m}}=\sqrt{2}\sigma_P^{\rm mid}/\eta$. For $N/2$ modulating cycles with total N shots measurements (N is even), the precision of $\varphi_{\rm m}$ can be expressed as

$$\sigma_{\varphi_{\rm m}}^{\rm FL}(N)=2\sigma_P^{\rm mid}/\eta\sqrt{N}, \tag{8}$$

where the superscript FL is the abbreviation of fringe locking.

For other types of noise, with the corresponding dependence of σ_{p_i} on the fringe site accounted for, $\sigma_{\varphi_{\rm m}}$ can also be estimated from Eq. (3) for the FSM, or from Eq. (8) for the FLM, and then the two can be compared.

3. In case of different noises

We consider three typical noises in atom interferometers to investigate their influence on the sensitivity. The extension to other noises is straightforward. The first one is the fringe-site independent noise as already analyzed in the previous section. This type of noise induces a fluctuation of the fringe offset; it may originate, for example, from the circuit noise in the detection system,[40] or the fluctuation of the background atoms number. The second one is the atom shot noise,[41] by which the induced variance is expressed as $\sigma_P=\sqrt{P(1-P)/N_{\rm at}}$ ($N_{\rm at}$ stands for the atoms number). This noise originates from the projection of the superposition state, and it is the ultimate precision limitation of atom interferometers using an incoherent atomic source. The third one is the phase noise, which happens in the interfering process, for example, the vibration noise, the Raman phase noise, *et al.*

For the fringe-site independent noise with a variance of $\sigma_P^{\rm off}$, according to Eqs. (5) and (8), the corresponding influences in the two modes are expressed as $\sigma_{\varphi_{\rm m}}^{\rm FS}(N)=2\sqrt{2}\sigma_P^{\rm off}/\eta\sqrt{N}$ and $\sigma_{\varphi_{\rm m}}^{\rm FL}(N)=2\sigma_P^{\rm off}/\eta\sqrt{N}$. It clearly shows that for identical N (namely, the same measurement time), the FLM allows us to gain an improvement factor of $\sqrt{2}$ on resolving $\varphi_{\rm m}$ over the FSM. The theoretical result for the FSM is confirmed by a numerical simulation, while that for the FLM is straightforward according to Eq. (8). In the simulation here, φ is uniformly scanned over 2π by 200 steps to form a fringe. It is expected that the approximation of substituting the summation by integral holds well in Eq. (4) with such a small step. p_i is thus calculated from Eq. (1) using pointed η and $\varphi_{\rm m}$ for each φ_i. To account for the fringe-site independent noise, we add to p_i numbers which are randomly drawn in a Gaussian distribution with constant standard deviation $\sigma_P^{\rm off}$. The precision of the obtained $\varphi_{\rm m}$ from 200 shots measurements (namely, $N=200$ for one full fringe) is estimated by the Allan deviation of 200 fitting results. The result is shown in Fig. 2, which is reported by the normalized precision $\sqrt{N}\sigma_{\varphi_{\rm m}}^{\rm FS,FL}(N)/\sigma_P^{\rm off}$.

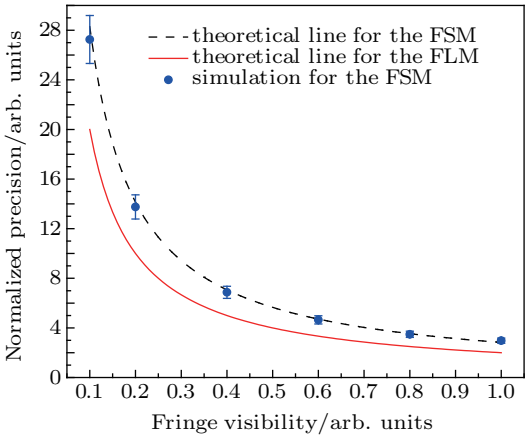


Fig. 2. (color online) Normalized precision for fringe-site independent noise. The theoretical result for the normalized precision $\sqrt{N}\sigma_{\varphi_{\rm m}}^{\rm FS,FL}(N)/\sigma_P^{\rm off}$ is $2\sqrt{2}/\eta$ in the FSM, and $2/\eta$ in the FLM. For the simulation here, $\sigma_P^{\rm off}=1.12\times10^{-3}$, and $\varphi_{\rm m}=1$ rad. The simulation for the FLM is not presented, since the result is straightforward according to Eq. (8).

For the atom shot noise with a variance of σ_φ, $\sigma_P=\sqrt{P(1-P)/N_{\rm at}}=\sqrt{P(1-P)}\sigma_P^{\rm shot}$, with a definition of $\sigma_P^{\rm shot}\equiv1/\sqrt{N_{\rm at}}$. In the FLM, it simply reduces to $\sigma_P^{\rm mid}=\sigma_P^{\rm shot}/2$. In the FSM, the precision can be obtained by Eq. (3), and it is

$$(\sigma_{\varphi_{\rm m}}^{\rm FS}(N))^2=\sum_{i=1}^{N}(\partial_{p_i}\varphi_{\rm m})^2(p_i(1-p_i)\sigma_P^{\rm shot})^2. \tag{9}$$

Approximating the summation by integral, the result is $\sigma_{\varphi_{\rm m}}^{\rm FS}(N)=\frac{\sqrt{2}\sigma_P^{\rm shot}}{\eta\sqrt{N}}\sqrt{1-\frac{1}{4}\eta^2}$. Thus for the atom shot noise, the improvement using the FLM is $\sqrt{2-\eta^2/2}$. It will gain a biggest improvement of $\sqrt{2}$ when η approaches 0, and a smallest improvement of $\sqrt{3/2}$ when η approaches 1. The numerical simulation further confirms this analysis, as shown in Fig. 3. For this simulation, the calculated p_i using Eq. (1) is added by a Gaussian distribution noise (with a constant standard deviation $\sigma_P^{\rm shot}$) multiplied by $\sqrt{p_i(1-p_i)}$, and the result is shown with unit $\sqrt{N}\sigma_{\varphi_{\rm m}}^{\rm FS,FL}(N)/\sigma_P^{\rm shot}$.

For the phase noises, $\sigma_P^2=\eta^2\sin^2(\varphi+\varphi_{\rm m})\sigma_\varphi^2/4$, where σ_φ denotes the variance of the phase noises. In the FLM, it simply reduces to $\sigma_P^{\rm mid}=\eta\sigma_\varphi/2$, which corresponds to $\sigma_{\varphi_{\rm m}}^{\rm FL}(N)=\sigma_\varphi/\sqrt{N}$. In the FSM, the precision can be estimated by Eq. (3) similarly for the atom shot noise, and the result is $\sigma_{\varphi_{\rm m}}^{\rm FS}(N)=\sqrt{3}\sigma_\varphi/\sqrt{2N}$. This result differs from the supposed $\sigma_{\varphi_{\rm m}}^{\rm FS}(N)=\sigma_\varphi/\sqrt{N}$, which is a consequence of the non-linear process for the cosine fitting. Thus for the phase noise, an improvement of a factor $\sqrt{3/2}$ is obtained using the FLM, which is independent of the fringe visibility. This result is also confirmed by a numerical simulation, as shown in Fig. 4. For this simulation, p_i is calculated based on Eq. (1) with $\varphi_{\rm m}$

added by a Gaussian distribution noise with standard deviation $\sigma_\varphi^{\rm shot}$. The result is shown in the unit of $\sqrt{N}\sigma_{\varphi_{\rm m}}^{\rm FS,FL}(N)/\sigma_\varphi$. We have noticed that in Ref. [42], the authors found that the simulated sensitivity for atom gradiometers is about 1.25 lower than the expected one after the common-mode rejects the vibration noise, which has not been explained. We note that the theoretical exact value should be $\sqrt{3/2}$, and this sensitivity degradation is caused by the FSM in the presence of phase noises.

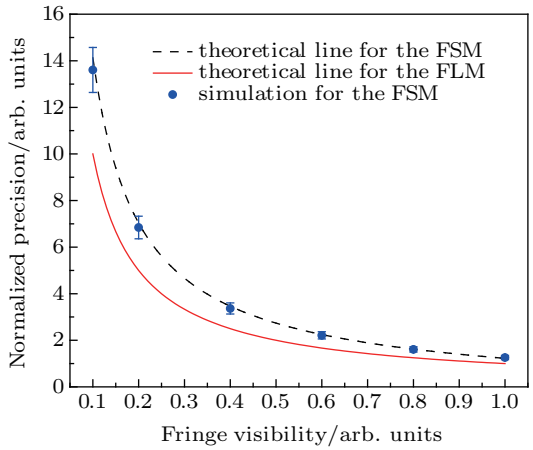


Fig. 3. (color online) Normalized precision for atom shot noise. The theoretical result for the normalized precision $\sqrt{N}\sigma_{\varphi_{\rm m}}^{\rm FS,FL}(N)/\sigma_P^{\rm shot}$ is $\sqrt{2-\eta^2/2}/\eta$ in the FSM, and $1/\eta$ in the FLM. For the simulation here, $N_{\rm at}=10^8$ (corresponding to $\sigma_P^{\rm shot}=1.12\times10^{-3}$), and $\varphi_{\rm m}=1$ rad.

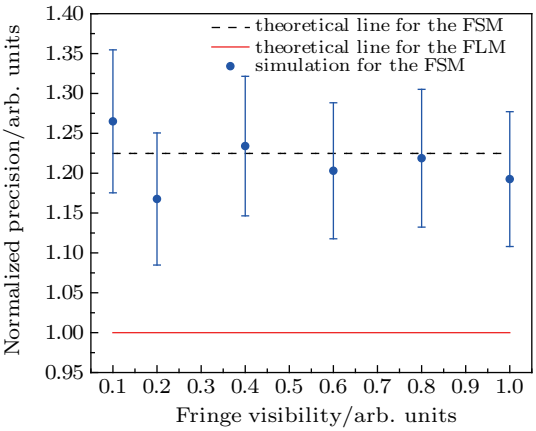


Fig. 4. (color online) Normalized precision for phase noise. The theoretical result for the normalized precision $\sqrt{N}\sigma_{\varphi_{\rm m}}^{\rm FS,FL}(N)/\sigma_\varphi$ is $\sqrt{3/2}$ in the FSM, and 1 in the FLM. For the simulation here, $\sigma_\varphi=1.12\times10^{-3}$ rad, and $\varphi_{\rm m}=1$ rad.

The analysis above shows that for the three kinds of noises, the FLM allows an improvement of the sensitivity in resolving the interferometry phase shift. It is thus advantageous to choose FLM over FSM in precision measurements. However, in experiments where the fringe visibility is the interested quantity,[43,44] the FSM should be adopted, since in the FLM the information of the real-time fringe amplitude is lost. In practice, the fringe amplitude must be known in advance by scanning the whole fringe. The fringe amplitude may drift in a long time. This drift problem can be resolved by occasionally switching back to the fringe-scanning mode to get a renewed fringe amplitude.

4. Coupled atom interferometers

In many applications, for example, in the determination of the gravitational constant G (see Ref. [12] for example), two interferometers are integrated to perform the desired measurements. It is expected to also be advantageous to explore the FLM in these applications. For two atom interferometers operated in differential modes, the dual fringes locking method has been adopted to ensure that the two interferometers are simultaneously operated at their respective mid-fringe.[45] This is realized by the feedback control of two independent controllable phases. For coupled atom interferometers, there is usually a common phase (denoted as $\varphi_{\rm c}$), for example, the Raman lasers phase in atom gravity gradiometers. It is convenient to dither the two atom interferometers synchronously by modulating this common phase. On the other hand, the other controllable phase (denoted as $\varphi_{\rm d}$) shall behave differently for the two interferometers. In the simplest case when $\varphi_{\rm d}$ only affects one of the two interferometers, for example, fringe I, $\varphi_{\rm c}$ is thus controlled to lock one fringe II, while $\varphi_{\rm d}$ is controlled to lock fringe I. Similar to the single interferometer, the appropriate values of $\varphi_{\rm c}$ and $\varphi_{\rm d}$ (denoted as $\varphi_{\rm c}^0$ and $\varphi_{\rm d}^0$, respectively) are firstly found to make $\varphi^{\rm I,II}\sim 2n^{\rm I,II}\pi$ at the same time (both $n^{\rm I}$ and $n^{\rm II}$ are integers, and $\varphi^{\rm I}=\varphi_{\rm c}+\varphi_{\rm d}+\varphi_{\rm m}^{\rm I}$ ($\varphi^{\rm II}=\varphi_{\rm c}+\varphi_{\rm m}^{\rm II}$) is the total phase shift for the respective interferometer). Then $\varphi_{\rm c}$ is modulated by $\pm\pi/2$. The corresponding transition probabilities for the two atom interferometers for every two consecutive shots can be expressed as

$$\begin{cases} P_{2l}^{\rm I,II}=(1-\eta^{\rm I,II}\cos(\varphi^{\rm I,II}-\pi/2))/2, \\ P_{2l+1}^{\rm I,II}=(1-\eta^{\rm I,II}\cos(\varphi^{\rm I,II}+\pi/2))/2, \end{cases} \tag{10}$$

where $\varphi_{\rm m}^{\rm I,II}$ denotes the phase shift induced by the interested quantity of the respective interferometer, and $\eta^{\rm I,II}$ denotes the corresponding fringe visibility. According to the linear approximation of Eq. (10) at the mid-fringe, the correction for feedback can be expressed as

$$\begin{cases} \delta(\varphi_{\rm c}^0)=-(P_{2l+1}^{\rm II}-P_{2l}^{\rm II})/\eta^{\rm II}, \\ \delta(\varphi_{\rm d}^0)=-(P_{2l+1}^{\rm I}-P_{2l}^{\rm I})/\eta^{\rm I}+(P_{2l+1}^{\rm II}-P_{2l}^{\rm II})/\eta^{\rm II}. \end{cases} \tag{11}$$

Once the corrections are made to form a closed feedback loop, the equation $\varphi^{\rm I,II}=2n^{\rm I,II}\pi$ is supposed to be tenable, from which the differential phase shift $\Delta\Phi\equiv\varphi_{\rm m}^{\rm I}-\varphi_{\rm m}^{\rm II}=\varphi_{\rm d}^0+2(n^{\rm I}-n^{\rm II})\pi$ can be deduced. Thus the value of the differential phase shift between the coupled atom interferometers can be obtained from the recorded value of $\varphi_{\rm d}^0$. Equation (11) also implies that the common variation of the two interferometers is compensated by the correction of $\varphi_{\rm c}^0$, while $\varphi_{\rm d}^0$ is adjusted to compensate the differential variation.

For independent noises between the two interferometers, the improvement of the sensitivity in resolving the differential phase shift by the FLM over that by the FSM is the same as that in the single interferometer for the three kinds of noise. For common phase noise, in the FSM, it can be suppressed by combining the two fringes to perform ellipse fitting[46] or Bayesian estimation.[47,48] In the FLM, the differential phase shift is also immune to the common phase noise, which is straightforward according to the correction of $\varphi_{\rm d}^0$ in Eq. (11).

For common fringe-site independent noise, the precision of the differential phase shift in the two approaches can be estimated by

$$\begin{cases} \sigma_{\Delta\Phi}^{\rm FS}(N) = \dfrac{2\sqrt{2}\sigma_P^{\rm off}}{\sqrt{N}}\sqrt{\dfrac{1}{(\eta^{\rm I})^2}+\dfrac{1}{(\eta^{\rm II})^2}-\dfrac{2\cos(\Delta\Phi)}{\eta^{\rm I}\eta^{\rm II}}}, \\ \sigma_{\Delta\Phi}^{\rm FL}(N) = \dfrac{2\sigma_P^{\rm off}}{\sqrt{N}}\left|\dfrac{1}{\eta^{\rm I}}-\dfrac{1}{\eta^{\rm II}}\right|. \end{cases} \tag{12}$$

The deduction of the precision for the FSM is detailed in Appendix A, while that for the FLM is straightforward according to Eq. (11). It is obvious that the suppression of the common offset noise in the FSM is dependent on both the fringe visibility and $\Delta\Phi$. When $\Delta\Phi$ equals to $2n\pi$ (n is an integer), the best suppression is achieved for the FSM. Even in that special situation, the suppression of the common offset noise using the FLM is still $\sqrt{2}$ better than that using the FSM. This conclusion is further confirmed by a numerical simulation, which is shown in Fig. 5. Actually, an improvement of about 3 times for the sensitivity has been demonstrated using the dual-fringe-locking method in our previous work.[45] It is worth noting that in the special case where $\eta^{\rm I}=\eta^{\rm II}$, the differential phase would not be influenced by this common noise using the FLM.

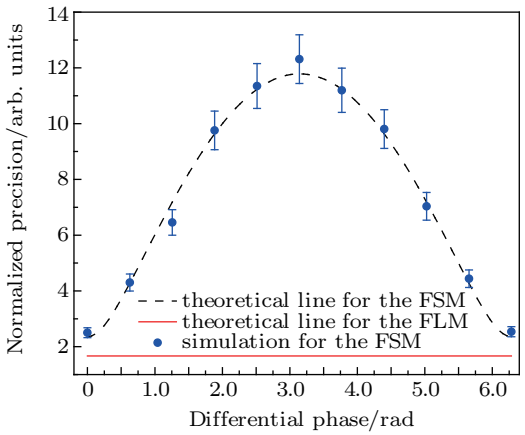


Fig. 5. (color online) Normalized precision for common fringe-site independent noise in coupled interferometers. The theoretical result for the normalized precision $\sqrt{N}\sigma_{\Delta\Phi}^{\rm FS,FL}(N)/\sigma_P^{\rm off}$ is $2\sqrt{2/(\eta^{\rm I})^2+2/(\eta^{\rm II})^2-4\cos(\Delta\Phi)/\eta^{\rm I}\eta^{\rm II}}$ in the FSM, and $|2/\eta^{\rm I}-2/\eta^{\rm II}|$ in the FLM. In this simulation, $\sigma_P^{\rm off}=1.12\times10^{-3}$, $\eta^{\rm I}=0.4$, $\eta^{\rm II}=0.6$, and $\varphi_{\rm m}^{\rm I}=0$ rad.

We also note that the FLM is capable of making some noises become common for the two interferometers, since in the fringe-locking mode, the two interferometers become completely synchronous. For example, the fluctuation induced by the relative intensity variation of the two detection beams in the normalized detection is $\delta_P=P(1-P)\delta_\alpha/\alpha$, where α denotes the intensity ratio of the two detection beams (e.g., Ref. [40]). While the fluctuation of the intensity ratio may be common for coupled atom interferometers, the transition probabilities of the two interferometers are usually different and vary when scanning $\varphi_{\rm c}$. However, in the FLM, the interferometers are operated at their respective mid-fringe, and thus the transition probabilities are nearly fixed, which both equal to $\delta_\alpha/4\alpha$ in the ideal case. Then in the FLM, the suppression of this noise is similar to that of the common offset noise.

We note that the FLM may find important applications in space-borne gravity gradiometers by atom interferometry, which are supposed to be core sensors in future satellite gravity measurement. On one hand, the promise of improving the sensitivity allows for a more precision observation of Earth's gravity field. On the other hand, compared with the FSM, the FLM allows a faster sampling rate, which is expected to help improve the space resolution (since the satellite orbits the Earth at a quite fast speed, typically 7.8 km/s).

5. Discussion and conclusion

Both in the analysis and simulation, the step in scanning a full fringe in the FSM is assumed to be so small that the summation can be approximated by the integral. In practical measurements, it is typical to scan tens of steps to obtain a full fringe. The simulation with 40 steps for sweeping a fringe over 2π is also performed. The result is well compatible with that using 200 steps. In addition to the cosine shape, the side locking strategy can also be applied to other nonlinear shapes. For example, in Ref. [49], a Gaussian shape is obtained by scanning the amplitude modulation frequency, and the Bloch frequency is extracted by the Gaussian fitting. By locking the measurements at the two sides of the Gaussian shape, an order of magnitude improvement of the sensitivity is achieved in their work. This work may provide hints for the theoretical investigation on the locking strategy in these shapes.

In conclusion, we have compared the corresponding sensitivities between the FSM and the FLM when suffering different noises in atom interferometers. In a single interferometer, the influences of three typical noises using the two methods are analyzed, and it is straightforward to extend to other noises. According to the analysis, the FSM will damage the sensitivity while the FLM allows an improvement of the sensitivity, which comes at the price of losing the information of the real-time fringe amplitude. In coupled interferometers, the FLM forces the two interferometers to be completely synchronous, and thus both the common phase noises and the common fringe-site independent noises can be suppressed.

Appendix A

The deduction of the precision of $\varphi_{\rm m}$ using cosine fitting based on the LSR method is present here. For a single fringe, the goal fitting function is $p_i = (1-\eta\cos(\varphi_i+\varphi_{\rm m}))/2$. According to Eq. (2), the algebraic value of η and $\varphi_{\rm m}$ is deduced from the following equations:

$$\begin{cases} \partial_\eta \left(\sum\limits_{i=1}^{N} \left((1-\eta\cos(\varphi_i+\varphi_{\rm m}))/2 - p_i\right)^2 \right) = 0, \\ \partial_{\varphi_{\rm m}} \left(\sum\limits_{i=1}^{N} \left((1-\eta\cos(\varphi_i+\varphi_{\rm m}))/2 - p_i\right)^2 \right) = 0. \end{cases} \tag{A1}$$

From the perfect differential of Eq. (A1) the partial differential $\partial_{p_i}\varphi_{\rm m}$ can be obtained by eliminating the differential related to η. With the second order variation of P neglected, the result is

$$\frac{\partial\varphi_{\rm m}}{\partial p_i} = \frac{M_{11}F_{i2} - M_{12}F_{i1}}{M_{11}M_{22} - M_{12}M_{21}}, \tag{A2}$$

where $\boldsymbol{F}$ is the partial derivatives matrix, and $\boldsymbol{M}$ is the variance-covariance matrix. The elements of the $N\times 2$ matrix $\boldsymbol{F}$ in the first and the second columns are $F_{i1} \equiv \partial_\eta P\big|_{\varphi=\varphi_i} = -\cos(\varphi_i+\varphi_{\rm m})/2$ and $F_{i2} \equiv \partial_{\varphi_{\rm m}} P\big|_{\varphi=\varphi_i} = \eta\sin(\varphi_i+\varphi_{\rm m})/2$, respectively. The $\boldsymbol{M}$ is defined as $\boldsymbol{M} \equiv \boldsymbol{F}^{\rm T}\boldsymbol{F}$. When assuming that φ is uniformly scanned over 2π with such an infinitesimal step that the summation can be approximated by an integral, equation (A2) is reduced to

$$\partial_{p_i}\varphi_{\rm m} = 4\sin(\varphi_i+\varphi_{\rm m})/\eta N. \tag{A3}$$

For coupled interferometers, the precision of deducing $\Delta\Phi = \varphi_{\rm m}^{\rm I} - \varphi_{\rm m}^{\rm II}$ can be calculated by

$$\sigma_{\Delta\Phi}^2 = \sum_{i=1}^{N}\left(\frac{\partial\Delta\Phi}{\partial p_i}\right)^2\sigma_{P_i}^2 = \sum_{i=1}^{N}\left(\frac{\partial\varphi_{\rm m}^{\rm I}}{\partial p_i} - \frac{\partial\varphi_{\rm m}^{\rm II}}{\partial p_i}\right)^2\sigma_{P_i}^2, \tag{A4}$$

where only the common variation of p_i for the coupled interferometers is considered. Substituting $\partial_{p_i}\varphi_{\rm m}^{\rm I,II}$ calculated from Eq. (A2) for each fringe into Eq. (A4), the precision of $\Delta\Phi$ can be further calculated. For the common offset noise, the variation of each p_i is independent and the variance is the same. Then the precision of $\Delta\Phi$ using FSM can be calculated from Eq. (A4) in the approximation of substituting the summation by integral, and the result is exactly Eq. (12).

References

[1] Weiss D S, Young B C and Chu S 1994 *Appl. Phys. B* **59** 217
[2] Wicht A, Hensley J M, Sarajlic E and Chu S 2002 *Phys. Scripta* **T102** 82
[3] Cladé P, de Mirandes E, Cadoret M, *et al.* 2006 *Phys. Rev. Lett.* **96** 033001
[4] Müller H, Chiow S W, Long Q, Vo C and Chu S 2006 *Appl. Phys. B* **84** 633
[5] Cadoret M, de Mirandes E, Cladé P, *et al.* 2008 *Phys. Rev. Lett.* **101** 230801
[6] Fixler J B, Foster G T, McGuirk J M and Kasevich M A 2007 *Science* **315** 74
[7] Lamporesi G, Bertoldi A, Cacciapuoti L, Prevedelli M and Tino G M 2008 *Phys. Rev. Lett.* **100** 050801
[8] Stuhler J, Fattori M, Petelski T and Tino G M 2003 *J. Opt. B: Quantum Semiclass. Opt.* **5** S75
[9] Bertoldi A, Lamporesi G, Cacciapuoti L, *et al.* 2006 *Eur. Phys. J. D* **40** 271
[10] Sorrentino F, Lien Y H, Rosi G, Cacciapuoti L, Prevedelli M and Tino G M 2010 *New J. Phys.* **12** 095009
[11] Fattori M, Lamporesi G, Petelski T, Stuhler J and Tino G M 2003 *Phys. Lett. A* **318** 184
[12] Rosi G, Sorrentino F, Cacciapuoti L, Prevedelli M and Tino T M 2014 *Nature* **510** 518
[13] Dimopoulos S, Graham P W, Hogan J M, Kasevich M A and Rajendran S 2008 *Phys. Rev. D* **78** 122002
[14] Bonnin A, Zahzam N, Bidel Y and Bresson A 2013 *Phys. Rev. A* **88** 043615
[15] Gaaloul N, Ahlers H, Schulze T A, *et al.* 2010 *Acta Astronautica* **67** 1059
[16] Dimopoulos S, Graham P W, Hogan J M, Kasevich M A and Rajendran S 2009 *Phys. Lett. B* **678** 37
[17] Tarallo M G, Mazzoni T, Poli N, Sutyrin D V, Zhang X and Tino G M 2014 *Phys. Rev. Lett.* **113** 023005
[18] Clairon A, Laurent P, Santarelli G, *et al.* 1995 *IEEE Trans. Instrum.* **44** 128
[19] Levi F, Lorini L, Calonico D and Godone A 2004 *IEEE Trans. Ultrason. Ferroelectrics Freq. Control* **51** 1216
[20] Wynands R and Weyers S 2005 *Metrologia* **42** S64
[21] Vian C, Rosenbusch P, Marion H, *et al.* 2005 *IEEE Trans. Instrum. Meas.* **54** 833
[22] Szymaniec K, Park S E, Marra G and Chalupczak W 2010 *Metrologia* **47** 363
[23] Gerginov V, Nemitz N, Weyers S, Schröder R, Griebsch D and Wynands R 2010 *Metrologia* **47** 65
[24] Heavner T P, Donley E A, Levi F, *et al.* 2014 *Metrologia* **51** 174
[25] Zhou M K, Hu Z K, Duan X C, *et al.* 2010 *Phys. Rev. A* **82** 061602
[26] Hu Z K, Duan X C, Zhou M K, *et al.* 2011 *Phys. Rev. A* **84** 013620
[27] Peters A, Chung K Y and Chu S 1999 *Nature* **400** 849
[28] Peters A, Chung K Y and Chu S 2001 *Metrologia* **38** 25
[29] Le Gouët J, Mehlstäubler T E, Kim J, Merlet S, Clairon A, Landragin A and Dos Santos F P 2008 *Appl. Phys. B* **92** 133
[30] Hauth M, Freier C, Schkolnik V, Senger A, Schmidt M and Peters A 2013 *Appl. Phys. B* **113** 49
[31] Müller H, Chiow S W, Herrmann S and Chu S 2008 *Phys. Rev. Lett.* **100** 031101
[32] Zhou M K, Pelle B, Hilico A and dos Santos F P 2013 *Phys. Rev. A* **88** 013604
[33] Bidel Y, Carraz O, Charrière R, Cadoret M and Zahzam N 2013 *Appl. Phys. Lett.* **102** 144107
[34] Altin P A, Johnsson M T, Negnevitsky V, *et al.* 2013 *New J. Phys.* **15** 023009
[35] Zhou M K, Hu Z K, Duan X C, *et al.* 2012 *Phys. Rev. A* **86** 043630
[36] Hu Z K, Sun B L, Duan X C, *et al.* 2013 *Phys. Rev. A* **88** 043610
[37] Cheinet P, Dos Santos F P, Petelski T, *et al.* 2006 *Appl. Phys. B* **84** 643
[38] Merlet S, Le Gouët J, Bodart Q, *et al.* 2009 *Metrologia* **46** 87
[39] Bevington P R and Robinson D K 2003 *Data Reduction and Error Analysis for the Physical Sciences* (3rd edn.) (New York: McGraw-Hill) p. 102
[40] Gauguet A, Canuel B, Lévèque T, Chaibi W and Landragin A 2009 *Phys. Rev. A* **80** 063604
[41] Itano W M, Bergquist J C, Bollinger J J, *et al.* 2009 *Phys. Rev. A* **47** 3554
[42] Dos Santos F P 2015 *Phys. Rev. A* **91** 063615
[43] Kellogg J R, Yu N, Kohel J M, Thompson R J, Aveline D C and Maleki L 2007 *J. Mod. Opt.* **54** 2533
[44] Lan S Y, Kuan P C, Estey B, Haslinger P and Muller H 2012 *Phys. Rev. Lett.* **108** 090402
[45] Duan X C, Zhou M K, Mao D K, *et al.* 2014 *Phys. Rev. A* **90** 023617
[46] Foster G T, Fixler J B, McGuirk J M and Kasevich M A 2002 *Opt. Lett.* **27** 951
[47] Stockton J K, Wu X and Kasevich M A 2007 *Phys. Rev. A* **76** 033613
[48] Varoquaux G, Nyman R A, Geiger R, *et al.* 2009 *New J. Phys.* **11** 113010
[49] Tarallo M G, Mazzoni T, Poli N, *et al.* 2014 *Phys. Rev. Lett.* **113** 023005